Fast power flow scheduling and sensitivity analysis for sizing a microgrid with storage

Rémy Rigo-Mariani, Bruno Sareni, Xavier Roboam

Fast power flow scheduling and sensitivity analysis for sizing a microgrid with storage

R. Rigo-Mariani[a,*], B. Sareni[b], X. Roboam[b]

[a] *University of Washington, Department of Electrical Engineering, 185 Stevens Way, 98195 Seattle, WA, United States*
[b] *Université de Toulouse, LAPLACE, UMR CNRS-INPT-UPS, site ENSEEIHT, 2 rue Camichel, 31 071 Toulouse, France*

Abstract

This article proposes a fast strategy for optimal dispatching of power flows in a microgrid with storage. The investigated approach is based on the use of standard mixed integer linear programming (MILP) algorithm in association with a coarse linear model of the microgrid. The resulting computational time is compatible with simulations over long periods of time allowing the integration of seasonal and stochastic features related to renewable energies. By using this fast scheduling strategy over a complete year of simulation, the microgrid cost effectiveness is considered. Finally, a sensitivity analysis is carried out in order to identify the most influent parameters that should be considered in a sizing loop. Different microgrid configurations are also investigated and compared in terms of cost-effectiveness.

Keywords: Smart grid; Storage; Optimal power dispatching; Mixed integer linear programming; Sensitivity analysis

0. Introduction

With the growing number of renewable energy sources the power grid topology has evolved and it could be now described as an aggregation of several microgrids both consumer and producer [8]. For those "prosumers", a classical strategy consists in selling all the highly subsidized production at important prices while all consumed energy is purchased [7]. Smarter operations become possible with the development of energy storage technologies and evolving price policies [28]. Those operations would aim at reducing the electrical bill taking account of consumption and production forecasts as well as the different fares and possible constraints imposed by the power supplier [10,14]. The microgrid considered in the paper is composed of a set of industrial buildings and factory with a subscribed power P_s of 156 kVA and a PV generator with a peak power of 175 kW (Fig. 1(a)). A 100 kW/100 kWh storage consisting in the association of ten high-speed flywheels is also introduced.

The strategy chosen to manage the overall system is based on a daily off-line optimal scheduling of power flows for the day ahead. Then, in real time, an on-line procedure adapts the same power flows in order to correct errors between forecasts and actual measurements [22]. Thus prediction for both consumption [3] and production [13] is a very

* Corresponding author.
E-mail addresses: rigor@uw.edu (R. Rigo-Mariani), sareni@laplace.univ-tlse.fr (B. Sareni), roboam@laplace.univ-tlse.fr (X. Roboam).

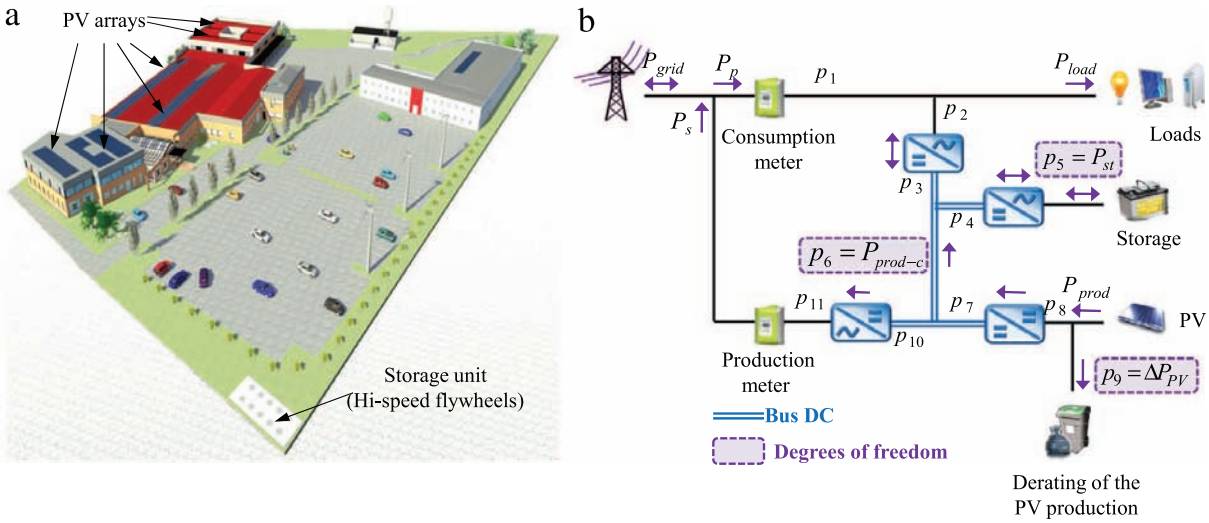

Fig. 1. Considered microgrid—(a) implementation site—(b) power flow model.

important issue in microgrid management problems but it is not considered here. Several algorithms have been investigated in previous works [23] to perform the off-line optimization for a single day. In particular, trust-region-reflective algorithm [9], clearing procedure [18], particular swarm optimization [15] and Dynamic Programming [4,20] have been compared in this context. But the high computational times observed did not comply with a sizing procedure that would require many runs of the procedure over long periods of time (e.g., weeks, months, years). The present study focuses on a faster approach consisting in two steps. Firstly, a basic Mixed Integer Linear Programming (MILP) algorithm solves the cost minimization problem with a coarse linear model of the system as in [24,17]. Then, a second procedure adapts the obtained solutions to comply with the requirements of a finer nonlinear model. The paper is organized as follows. Section 1 describes the nonlinear model of the system with the various losses taken into account. The text also refers to the optimization problem that aims at minimizing the electrical bill for the day ahead with the forecast for the production, consumption and prices. Then, Section 2 presents the fast optimization approach with the hypothesis considered for the coarse model. A particular attention is attached to the introduction of integer variable to consider the exceeding of subscribe power. Finally, the adaptation of the control references resulting from the MILP optimization is described. In Section 3, the results obtained for two test days are presented with or without considering grid constraints. The last section uses the developed algorithm to investigate different sizings of the microgrid with regard to the yearly cost. Finally, a sensitivity analysis is performed in order to estimate the most significant parameters that should be considered in a sizing procedure.

1. Nonlinear model of the studied microgrid

1.1. Power flow model

As illustrated in Fig. 1(b), the components are connected though a common DC bus. Voltages and currents are not considered so far. The microgrid sizing (cable length) is very limited. Thus losses within the lines can be aggregated with converter efficiencies. Furthermore, the paper focuses on the optimal scheduling of the system without considering a real-time management strategy (i.e. voltage/current control). The approach is "in power" with a study referring to the optimization of active power flows $p_i(t)$. A nomenclature of the used symbols is given on Table 1. Due to the grid policy, three constraints have to be fulfilled at each time step t. The power flows thought the meters have to remain unidirectional (i.e. $P_c(t) \geq 0$ and $P_p(t) \geq 0$). In addition, $P_{prod\text{-}c}(t) \geq 0$ to avoid illegal use of the storage device, it cannot discharge itself through the production meter. The equations between all power flows are generated using the graph theory and the incidence matrix [6]. As illustrated in Fig. 1(b), three degrees of freedom are required to manage the whole system knowing production and consumption:

- $p_5(t) = P_{st}(t)$: the power flowing from/to the storage unit (defined as positive for discharge power)
- $p_6(t) = P_{prod\text{-}c}(t)$: the power flowing from the PV arrays to the common DC bus

Table 1
List of the used symbols.

P_{load}	Consumed power	kW
P_{prod}	Solar PV production	kW
p_i	Power flows used to characterize the system (Section 2.1)	kW
P_p	Power flowing through the consumption meter	kW
P_s	Power flowing through the production meter	kW
P_{st}	Power flowing from/to the storage unit	kW
P_{FS}	Power flowing from/to the flywheel with losses	kW
P_{st_min}, P_{st_max}	Lower and upper bounds for P_{st}	kW
E_{FS}	Maximum stored energy in the storage unit	kWh
K_{FS}	Self-discharge coefficient of the flywheels (Section 2.3)	kWh/h
η_{FS}	Flywheels efficiency depending on P_{st}	–
SOC	State of charge of the storage unit	%
$SOC_{\min}$, $SOC_{\max}$	Lower and upper bounds for the SOC level	%
SOC_{start}, SOC_{end}	Initial and final daily values for the SOC level	%
P_{PV}	Nominal power of the photovoltaic generator	kWc
$P_{prod\text{-}c}$	Amount of solar production self consumed	kW
ΔP_{PV}	Solar production derated in case of microgrid congestion	kW
P_{grid}	Power flowing between the main grid and the microgrid	kW
P_{grid_min}, P_{grid_max}	Lower and upper bounds for P_{grid}	kW
$\eta_{CVS,i}$	Efficiency of the ith converter in the graph representation	–
C_p	Cost for the purchased energy	€/kWh
C_s	Cost for the sold energy	€/kWh
C_{ex}	Cost to penalized the exceeding of P_s	€/h
t	Time step	h
$\mathbf{P_{ref}}$	Matrix/vector with optimization variables	–
$C(\mathbf{P_{ref}})$	Daily cost to be minimized by the optimization algorithm	€
$\mathbf{C_{nl}}$	Vector with the nonlinear constraints	–

- $p_9(t) = \Delta P_{PV}$ denotes the possibility to decrease the PV production (MPPT degradation) in order to fulfill possible grid constraints., in particular when the power supplier does not allow (or limits) the injection of the PV production into the main grid (ΔP_{PV} is normally set to zero).

Note that load control is not investigated in the study but could also be considered in further works as an additional degree of freedom with the possibility of shedding or delaying some consumption. A particular attention is also paid to the grid power $P_{grid}(t)$ which should comply with requirements possibly set by the power supplier (Eqs. (1) and (2))

$$P_{grid}(t) = P_c(t) - P_p(t) \tag{1}$$

$$P_{grid\_min}(t) < P_{grid}(t) < P_{grid\_max}(t). \tag{2}$$

1.2. Efficiencies and nonlinear approach

A "fine model" is defined taking account of efficiencies of power converters (typically 98%) and storage losses. These losses are computed with the state of charge SOC (in%) and the power P_{st} using a function $P_{loss}(SOC)$ and calculating the efficiency with a fourth degree polynomial $\eta_{FS}(P_{st})$ (Eq. (3)) depending on the direction of the power flow P_5 (i.e; charge or discharge conditions). Both P_{loss} and η_{FS} functions are extracted from measurements provided by the manufacturer.

$$P_{FS}(t) = P_{loss}\left(SOC(t)\right) + P_{st}(t) \times \eta_{FS}\left(p_{st}(t)\right). \tag{3}$$

Once the overall efficiency is computed, the true power P_{FS} associated with the flywheel is calculated as well as the SOC evolution using the maximum stored energy E_{FS} (in kWh), the time step Δt (typically 1 h for the off-line optimization) and the control reference P_{st} (Eq. (4)).

$$SOC(t + \Delta t) = SOC(t) - \frac{P_{FS}(t)}{E_{FS}} \times \Delta t \times 100. \tag{4}$$

Another coefficient K_{FS} (in kWh/h) is also introduced to estimate the self-discharge of the flywheels when they are not used (i.e. $P_{st} = 0$) (Eq. (5)).

$$SOC(t + \Delta t) = SOC(t) - \frac{K_{FS}}{E_{FS}} \times \Delta t \times 100. \tag{5}$$

1.3. Optimal power dispatching problem

As previously explained, the objective of the off-line dispatching is to minimize the electrical bill for the day ahead. This minimization is performed from the production and consumption forecasts and by considering the grid constraints and the prices of the purchased (C_p) and the sold (C_s) energies. Overshoots with regard to the subscribed power P_s are penalized with a cost C_{ex} expressed in € per hour. The references of the power flows associated with the degrees of freedom are computed on the overall day in a vector $\mathbf{P_{ref}}$ with 72 variables (i.e. 3×24 with a time step $\Delta t = 1$ h). Once $\mathbf{P_{ref}}$ is determined, all other power flows are computed with the forecasted values of consumption and production. Then $\mathbf{P_c}$ and $\mathbf{P_p}$ are known and the cost function is calculated as in Eq. (6) for a 24 h simulated period. That cost function $C(\mathbf{P_{ref}})$ is defined as the difference between purchased and sold energy plus the amount of penalties due to the exceeding of subscribed power.

$$C(\mathbf{P_{ref}}) = \sum_{t=0}^{24\text{ h}} P_c(t) \times C_c(t) - P_p(t) \times C_p(t) + \delta(t) \times C_{ex} \quad \text{with} \begin{cases} \delta(t) = 0 & \text{if } P_c(t) < P_s \\ \delta(t) = 1 & \text{if } P_c(t) > P_s. \end{cases} \tag{6}$$

In previous works, several algorithms were applied in order to solve the dispatching problem with the fine model [9]. Firstly, a trust-region-reflective algorithm (TR) has been used. This method aims at solving the problem by approximating the objective function with a simpler quadratic function in a trust-region area [9]. From an initial starting solution, the procedure minimizes the cost while fulfilling all the nonlinear constraints computed in a vector $\mathbf{c_{nl}}$ (Eq. (7)).

$$\mathbf{P^*_{ref}} = \left[\mathbf{P^*_{st}} \quad \mathbf{P^*_{prod\text{-}c}} \quad \mathbf{\Delta P^*_{PV}}\right] = \arg\min\left(C(\mathbf{P_{ref}})\right) \quad \text{with } \mathbf{c_{nl}}(\mathbf{P^*_{ref}}) \leq 0. \tag{7}$$

Stochastic methods are then considered with, a Genetic Algorithm with a clearing procedure which preserves diversity in the population (CL) [18] and a Particle Swarm Optimization (PSO) procedure [15]. All constraints related to power flows are included in the cost function with a classical exterior penalty approach. The algorithm returns the best individual in the population from a given number of generations (Eq. (8)).

$$\mathbf{P^*_{ref}} = \left[\mathbf{P^*_{st}} \quad \mathbf{P^*_{prod\text{-}c}} \quad \mathbf{\Delta P^*_{PV}}\right] = \arg\min\left(C(\mathbf{P_{ref}}) + \lambda \times \sum_i \mathbf{c_{nl}}(i)\right) \tag{8}$$

where the penalty factor λ is set to a sufficiently high value (typically 10^6) in order to ensure constraints fulfillment.

Finally, an original self-adaptive approach based on dynamic programming (DP) [4] has been developed in [22] and is denoted as DPa. It consists in a step by step minimization of the storage *SOC* levels, sampled on the overall range (i.e. [0%–100%]) with given accuracy ΔSOC [20]. The complexity and performance of this algorithm depend on this *SOC* sampling that determines the number of studied states.

2. Linear model and fast optimization procedure

2.1. Definition of a coarse linear model

In a second step, a coarse model is developed in order to speed up the solving by using a linear formulation of the problem. Firstly, the converter efficiencies are neglected which leads to the reduction of the number of power flows used to describe the system (Eq. (9)).

$$\begin{cases} p_2(t) = p_3(t) \\ p_4(t) = p_5(t) \\ p_7(t) = p_8(t) \\ p_{10}(t) = p_{11}(t). \end{cases} \tag{9}$$

In this model, storage losses are also neglected as well as the self-discharge. Thus, the *SOC* is simply computed at each time step of duration $\Delta t = 1$ h (Eq. (10))

$$SOC(t+\Delta t) = SOC(t) - \frac{P_{st}(t)}{E_{FS}} \times \Delta t \times 100. \tag{10}$$

2.2. *Mixed integer linear programming applied to a coarse model*

Even if all power flows p_i are linearly expressed with the degrees of freedom it is not possible to use standard Linear Programming (LP). Indeed, taking the exceeding of subscribed power into account is strongly nonlinear. An additional integer variable δ is included in the decision variable vector [5]. The values of δ is 0 or 1 depending on either the grid power exceeds the subscribed power or not (Eq. (6)). It becomes possible to solve the optimal problem expressed according to Eq. (11) using Mixed Integer Linear Programming (MILP).

$$\mathbf{P^*_{ref}} = \begin{bmatrix}\mathbf{P^*_{st}} & \mathbf{P^*_{prod\text{-}c}} & \mathbf{\Delta P^*_{PV}} & \mathbf{\delta^*}\end{bmatrix} = \arg\min\left(\mathbf{C_L}\cdot\mathbf{P_{ref}}\right) \quad \text{with } \mathbf{A}\cdot\mathbf{P^*_{ref}} \leq \mathbf{B}. \tag{11}$$

In this subsection, the coarse model is used to generate the cost function vector $\mathbf{C_L}$ as well as the constraints matrices and vectors ($\mathbf{A}$, $\mathbf{B}$) that are required to run the MILP as in Eq. (11). Firstly, the upper ($\mathbf{u_b}$) and lower ($\mathbf{l_b}$) bounds of the decision variables are expressed using the vector $\mathbf{J_n}$ with n coefficients equal to 1, where n is the number of simulated time steps, i.e. $n = 24$ for a whole day with $\Delta t = 1$ h (Eq. (12)). In particular, the limits of $\mathbf{P_{st}}$ refer to the maximum charge and discharge powers of the storage with $P_{st\_min} = -100$ kW and $P_{st\_max} = 100$ kW.

$$\begin{cases}\mathbf{l_b} = \begin{bmatrix}P_{st\_min} \times \mathbf{J_n} & 0 \times \mathbf{J_n} & 0 \times \mathbf{J_n} & 0 \times \mathbf{J_n}\end{bmatrix} \\ \mathbf{u_b} = \begin{bmatrix}P_{st\_max} \times \mathbf{J_n} & \mathbf{P_{prod}} & \mathbf{P_{prod}} & 1 \times \mathbf{J_n}\end{bmatrix}.\end{cases} \tag{12}$$

The previous cost function $C(\mathbf{P_{ref}})$ is developed for the coarse model in Eq. (13) according to the decision variables P_{st}, $P_{prod\text{-}c}$, ΔP_{PV} and δ. P_c and P_p are linearly dependent with the degrees of freedom. The nonlinear terms with P_{prod} and P_{load} are removed to obtain the vector $\mathbf{C_L}$ used in the MILP optimization (Eq. (14)).

$$C(\mathbf{P_{ref}}) = \sum_{t=0}^{24\text{ h}} \begin{pmatrix} -P_{st}(t) \times C_c(t) + P_{prod\text{-}c}(t) \times \big(C_p(t) - C_c(t)\big) + \Delta P_{PV}(t) \times C_p(t) + \delta(t) \times C_{ex} \\ + P_{load}(t) \times C_c(t) - P_{prod}(t) \times C_p(t) \end{pmatrix} \tag{13}$$

$$\mathbf{C_L}\cdot\mathbf{P_{ref}} = C(\mathbf{P_{ref}}) - \mathbf{P_{load}} \times \mathbf{C_c^T} + \mathbf{P_{prod}} \times \mathbf{C_p^T} \quad \text{with } \mathbf{C_L} = \begin{bmatrix}-\mathbf{C_c^T} & (\mathbf{C_p^T} - \mathbf{C_c^T}) & \mathbf{C_p^T} & \mathbf{C_{ex}} \times \mathbf{J_n}\end{bmatrix}. \tag{14}$$

The constraints matrix $\mathbf{A}$ and vector $\mathbf{B}$ are built by concatenating the matrices $\mathbf{A_i}$ and $\mathbf{B_i}$ used to express each grid requirement. In the following equations, the identity and zero matrices $n \times n$ are denoted as $\mathbf{I_n}$ and $\mathbf{0_n}$, and the lower triangular is $\mathbf{T_n}$. Some constraints in the microgrid are implicitly included in the bounds previously defined (e.g. the requirement $P_{prod\text{-}c}(t) \geqslant 0$). Eqs. (15) and (16) allow controlling the powers though the meters that have both to remain positive with the given convention.

$$\begin{cases}\mathbf{P_p} \geq 0 \Leftrightarrow P_{st}(t) + P_{prod\text{-}c}(t) \leq P_{load}(t) \quad \text{for } t \in [0..24\text{ h}] \\ \mathbf{A_1} \times \mathbf{P_{ref}} \leq \mathbf{B_1} \quad \text{with } \mathbf{A_1} = \begin{bmatrix}\mathbf{I_n} & \mathbf{I_n} & \mathbf{0_n} & \mathbf{0_n}\end{bmatrix} \text{ and } \mathbf{B_1} = \mathbf{P_{load}}\end{cases} \tag{15}$$

$$\begin{cases}\mathbf{P_s} \geq 0 \Leftrightarrow P_{prod\text{-}c}(t) + \Delta P_{PV}(t) \leq P_{prod}(t) \quad \text{for } t \in [0..24\text{ h}] \\ \mathbf{A_2} \times \mathbf{P_{ref}} \leq \mathbf{B_2} \quad \text{with } \mathbf{A_2} = \begin{bmatrix}\mathbf{0_n} & \mathbf{I_n} & \mathbf{I_n} & \mathbf{0_n}\end{bmatrix} \text{ and } \mathbf{B_2} = \mathbf{P_{PV}}.\end{cases} \tag{16}$$

The possible bounds set by the grid operator for P_{grid} are considered by summing all the overshoots. The negative and positive deviations are computed in Eqs. (17) and (18).

$$\begin{cases}\mathbf{P_{grid}} \geq \mathbf{P_{grid\_min}} \Leftrightarrow P_{st}(t) + P_{prod\text{-}c}(t) \leq P_{load}(t) - P_{prod}(t) - P_{grid\_min}(t) \quad \text{for } t \in [0..24\text{ h}] \\ \mathbf{A_3} \times \mathbf{P_{ref}} \leq \mathbf{B_3} \quad \text{with } \mathbf{A_3} = \begin{bmatrix}\mathbf{I_n} & \mathbf{0_n} & \mathbf{I_n} & \mathbf{0_n}\end{bmatrix} \text{ and } \mathbf{B_3} = \mathbf{P_{load}} - \mathbf{P_{prod}} - \mathbf{P_{grid\_min}}\end{cases} \tag{17}$$

$$\begin{cases}\mathbf{P_{grid}} \leq \mathbf{P_{grid\_max}} \Leftrightarrow -P_{st}(t) - \Delta P_{PV}(t) \leq P_{grid\_max}(t) - P_{load}(t) + P_{prod}(t) \quad \text{for } t \in [0..24\text{ h}] \\ \mathbf{A_4} \times \mathbf{P_{ref}} \leq \mathbf{B_4} \quad \text{with } \mathbf{A_4} = \begin{bmatrix}-\mathbf{I_n} & \mathbf{0_n} & -\mathbf{I_n} & \mathbf{0_n}\end{bmatrix} \text{ and } \mathbf{B_4} = \mathbf{P_{grid\_max}} - \mathbf{P_{load}} + \mathbf{P_{prod}}.\end{cases} \tag{18}$$

The storage SOC has to lie between 0% and 100% (Eqs. (19) and (20)). Furthermore, an additional constraint is introduced in order to force the SOC to return to its initial level, i.e. $SOC(24\text{ h}) = SOC(0) = 50\%$: in fact this equality constraint is indirectly set through the inequality of Eq. (21) and by means of the cost optimization which naturally leads to fully exploit (i.e. to discharge) the storage device. Using Eq. (10) for $t = 0$ h..24 h, the constraints are expressed as follows:

$$\begin{cases} \mathbf{SOC} \geq 0 \Leftrightarrow \displaystyle\sum_{i=0}^{i=t} P_{st}(i) \leq \frac{E_{FS}}{100} SOC(0) \quad \text{for } t \in [0..24\text{ h}] \\ \mathbf{A_5} \times \mathbf{P_{ref}} \leq \mathbf{B_5} \quad \text{with } \mathbf{A_5} = \begin{bmatrix} \mathbf{T_n} & \mathbf{0_n} & \mathbf{0_n} & \mathbf{0_n} \end{bmatrix} \text{ and with } \mathbf{B_5} = \dfrac{E_{FS}}{100} SOC(0) \times \mathbf{J_n} \end{cases} \tag{19}$$

$$\begin{cases} \mathbf{SOC} \leq 100 \Leftrightarrow -\displaystyle\sum_{i=0}^{i=t} P_{st}(i) \leq \frac{E_{FS}}{100} (100 - SOC(0)) \quad \text{for } t \in [0..24\text{ h}] \\ \mathbf{A_6} \times \mathbf{P_{ref}} \leq \mathbf{B_6} \quad \text{with } \mathbf{A_6} = \begin{bmatrix} -\mathbf{T_n} & \mathbf{0_n} & \mathbf{0_n} & \mathbf{0_n} \end{bmatrix} \text{ and with } \mathbf{B_6} = \dfrac{E_{FS}}{100} (100 - SOC(0)) \times \mathbf{J_n} \end{cases} \tag{20}$$

$$\begin{cases} SOC(24\text{ h}) \geq SOC(0) \Leftrightarrow \displaystyle\sum_{t=0}^{t=24\text{ h}} P_{st}(t) \leq 0 \\ \mathbf{A_7} \times \mathbf{X} \leq \mathbf{B_7} \quad \text{with } \mathbf{A_7} = \begin{bmatrix} \mathbf{J_n} & 0 \times \mathbf{J_n} & 0 \times \mathbf{J_n} & 0 \times \mathbf{J_n} \end{bmatrix} \text{ and } \mathbf{B_7} = 0. \end{cases} \tag{21}$$

Considering the penalties due to the overshoots when P_s is exceeded imposes the values for δ. That is performed using the constraint in Eq. (22) where M denotes the maximum expected value for $(P_1 - P_s)$ (set to 250 kVA here). Note that the constraint is expressed at each time step.

$$\begin{cases} (P_c(t) - P_s) - M.\delta(t) \leq 0 \Leftrightarrow -P_{st}(t) - P_{prod\text{-}c}(t) - M.\delta(t) \leq P_s - P_{load}(t) \\ \mathbf{A_8} \times \mathbf{P} \leq \mathbf{B_8} \quad \text{with } \mathbf{A_8} = \begin{bmatrix} -\mathbf{I_n} & -\mathbf{I_n} & \mathbf{0_n} & -M \times \mathbf{I_n} \end{bmatrix} \text{ and } \mathbf{B_8} = P_s \times \mathbf{J_n} - \mathbf{P_{load}}. \end{cases} \tag{22}$$

2.3. Correction of the obtained solutions

The MILP dispatching problem refers to a constraints matrix $\mathbf{A}$ with a great number of coefficients equal to 0. Thus the problem is implemented using sparse matrices [12] and the optimum is quickly found with an adapted solver such as GLPK [16]. The corresponding CPU time is less than one second on a particular day.

However, some preliminary results show that the obtained solutions obviously do not comply with the requirements of the first nonlinear microgrid model. Fig. 2 illustrates a case for which the solution $\mathbf{P^*_{ref}}$ obtained with MILP is simulated with the finer model equations. The resulting flow P_p through the production meter presents some forbidden negative values with small magnitudes (> -0.3 kW) (Fig. 2(a)). It should be noted that a deep discharge of the storage occurs at around 22 p.m. The SOC goes down to -15% with the finer model while it remains to 0% and fulfills the constraints with the coarse linear model. Taking account of the flywheels losses leads to a slowing down of the storage charge and a speeding up of the storage discharge

In the same way, the cost function returned by the coarse model is not correct. Therefore, the control references ($\mathbf{P_{refL}}$) related to the degrees of freedom obtained with the MILP in association with the coarse model should be adapted in order to comply with the finer microgrid model. This can be performed using a step by step correction which aims at minimizing the cost while fitting the SOC computed from the nonlinear model with the one resulting from the MILP optimization (denoted as SOC_L). At each time step t, the correction procedure is formulated as in Eq. (23) with ε set to a small value (typically $\varepsilon = 10^{-6}$).

$$\begin{cases} P^*_{ref}(t) = \begin{bmatrix} P^*_{st}(t) & P^*_{prod\text{-}c}(t) & \Delta P^*_{PV}(t) \end{bmatrix} = \arg\min \left(C \left(P_{ref}(t) \right) \right) \\ \quad \text{with } \mathbf{c^t_{nl}} \left(P^*_{ref}(t) \right) \leq 0 \text{ and } SOC_L(t + \Delta t) - \varepsilon \leq SOC(t + \Delta t) \leq SOC_L(t + \Delta t) + \varepsilon. \end{cases} \tag{23}$$

The cost function with the decision variables is computed similarly to (6) with the nonlinear model and the instantaneous bounds are inherited from Eq. (12). The instantaneous constraints $\mathbf{c^t_{nl}}$ refer to limits for P_{grid} and the requirements for the monodirectional flows through the meters (Eq. (24)). The constraints related to the SOC are

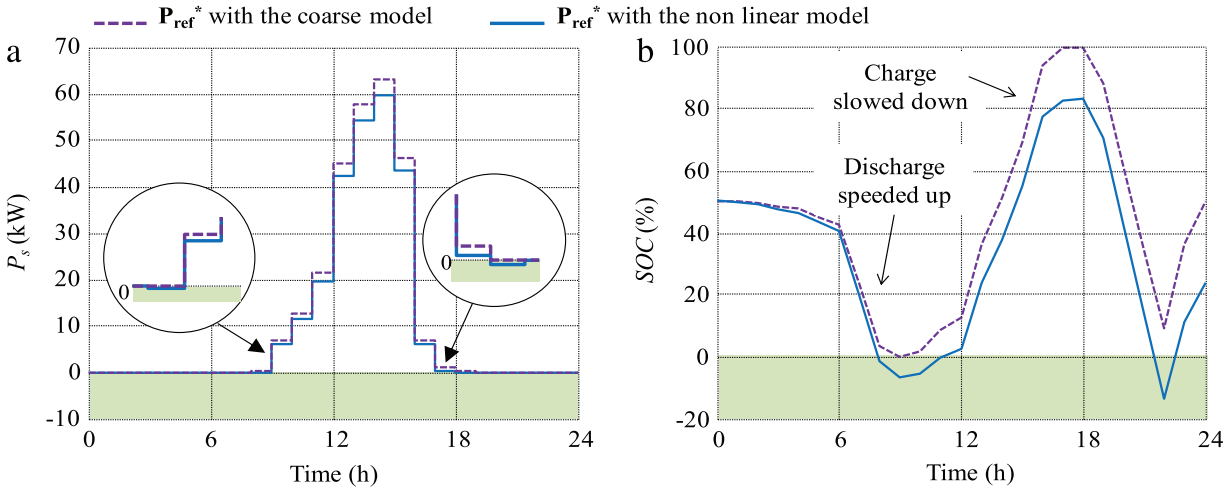

Fig. 2. Constraints violation for the finer nonlinear model—(a) P_s—(b) SOC.

added to the problem with two additional inequalities that have to remain below 0.

$$\mathbf{c_{nl}^t} = \begin{bmatrix} -p_1(t) \\ -p_{10}(t) \\ P_{grid}(t) - P_{grid\_max}(t) \\ P_{grid\_min}(t) - P_{grid}(t) \end{bmatrix}. \tag{24}$$

This local minimization problem is solved using the TR method as in Eq. (7) with a starting point equal to $P_{refL}(t)$. The convergence is ensured in a very short CPU time due to its small dimensionality (only three decision variables have to be determined). Note that the $P_{st}(t)$ decision variable is coupled with the desired SOC trajectory. It could lead in some cases to the non fulfillment of the grid constraints, e.g. if there is no production while the grid operator imposes a consumption to a given value $P_{grid}(t)$ different from $P_{load}(t)$. Thus $P_{prod\text{-}c}(t) = \Delta P_{PV}(t) = 0$ and then $P_{st}(t)$ should fed the difference $P_{grid}(t) - P_{load}(t)$. This value does not necessarily comply with the $P_{st}(t)$ reference which allows ensuring $SOC(t + \Delta t) = SOC_L(t + \Delta t)$. In such a situation the previous "instantaneous" optimization does not converge and is then rerun as in Eq. (25) with a SOC level between 0% and 100%.

$$\begin{cases} P_{ref}^*(t) = \left[P_{st}^*(t) \quad P_{prod\text{-}c}^*(t) \quad \Delta P_{PV}^*(t)\right] = \arg\min\left(C\left(P_{ref}(t)\right)\right) \\ \quad \text{with } \mathbf{c_{nl}^t}\left(P_{ref}^*(t)\right) \leq 0 \text{ and } 0 \leq SOC(t + \Delta t) \leq 100. \end{cases} \tag{25}$$

Typically, the CPU time related to this correction procedure is around three seconds over a day of simulation. The MILP algorithm associated with the previous correction procedure is denoted as MILP$_C$ in the following parts.

3. Test results over a day

3.1. Input data

Two test days are considered to compare the performances of the MILPc method with the results returned by the previous algorithm. The consumption profiles are extracted from data provided by the microgrid owner while the production estimation is based on solar irradiation forecasts, computed with a model of PV arrays [11]. The load and production profiles for the two tested days are presented in Fig. 3 with different amount of consumed or generated energies. The "spring day" corresponds to high values of irradiance and a low consumption with no overshoot with regard to the subscribed power P_s (set to156 kVA) (Fig. 3(a)). On the contrary, for the "winter day" P_s is exceeded during three hours from 3 to 6 p.m. with a penalized electrical bill (Fig. 3(b)).

Energy prices result from one of the fares proposed by the French main power supplier [27] increased by 30%. Thus, the purchase cost C_c has night and daily values with 10 c€/kWh from 10 p.m. to 6 a.m. and 17 c€/kWh otherwise. Sale fare C_p is set to 10 c€/kWh which corresponds to the price for such PV plants. $C_{ex} = 14$ €/h but the

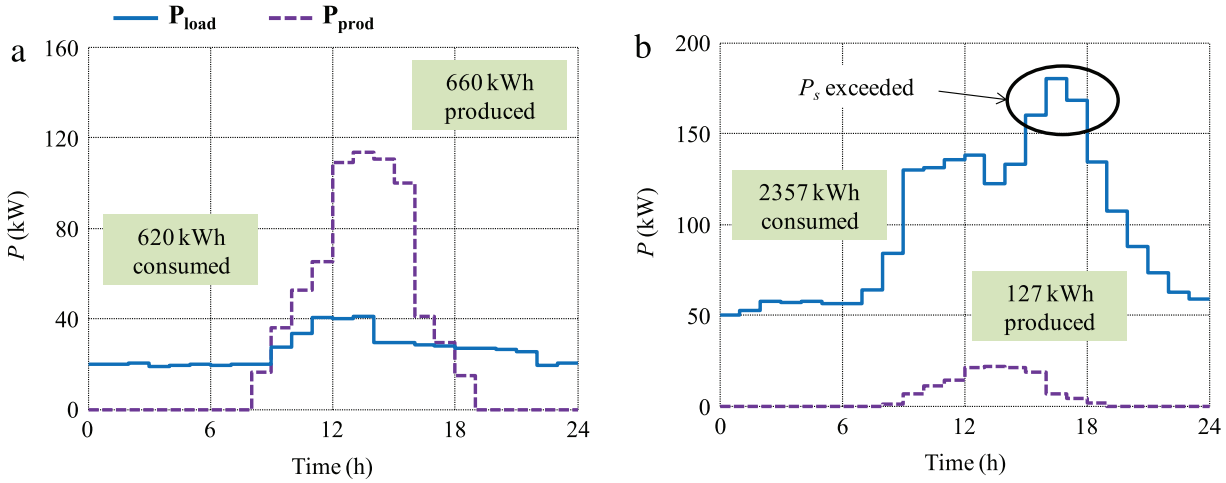

Fig. 3. Load and production forecasted profiles—(a) "spring day"—(b) "winter day".

Table 2
Results of the different algorithms for the "spring day".

Algorithm	TR	CL	PSO	DP	DPa	MILPc
$C(\mathbf{P}^*_{\mathbf{ref}})$ (€)	0.4	0.9	17.8	−0.6	−0.2	0.9
CPU Time	1 h	5 h	2 h	2 h	10 min	3 s

prices related to the subscribed power (subscription fee) is not considered yet. The PC used to implement and run the procedures has 8 GB of installed RAM and a processor of 3.2 GHz.

3.2. *"Spring day" and grid constraints*

The optimization algorithms are firstly tested regarding the "spring day" and compared in terms of final cost and CPU time. Grid constraints are considered with no consumption allowed during peak hours from 7 to 9 p.m. They are expressed according Eq. (26).

$$\begin{cases} P_{grid\_min}(t) = -10^3 \text{ kW} \quad \forall t \in 0\text{ h} \ldots 24\text{ h} \\ P_{grid\_max}(t) = 0 \text{ kW} \quad \text{for } t = 19\text{ h et } t = 20\text{ h and } P_{res\_max}(t) = 10^3 \text{ kW otherwise.} \end{cases} \tag{26}$$

The results returned from the procedures are advised in Table 2 and show a wide range of CPU times. Indeed the stochastic methods (i.e. CL and PSO) require a great number of evaluations for the objective function and led to a higher computational time. The best result is obtained in around 2 h with the basic DP and a small ΔSOC equal to 1%. That CPU time is reduced using the DPa but with a little higher cost. The MILPc is the fastest method and find an optimum similar to the solution return from the CL after 5 h of computation in only three seconds.

Fig. 4 shows the power grid profiles with and without storage associated to the optimal power dispatching (MILPc solution). Adding a storage device allows fulfilling the grid constraints. Flywheels are also used in order to reduce the electrical bill by adapting the energy balance between day and night. The storage is discharged at the beginning of the day in order to lower the cost when prices are higher (after 6 a.m.). Then the solar production feds the loads and charges the flywheels. At the end of the day the storage is fully used to satisfy the constraints before it returned to the desired value of 50% (Fig. 4(b)).

The cost analysis in Table 3 shows the advantages of the storage and optimal dispatching compared to a case denoted as INIT with no storage, where all the consumption is purchased from the grid while all the production is sold. The cost is mainly reduced because of the self consumed production during the day when prices for the purchased energy are higher. In particular, the fulfillment of grid constraints could be subsidized by the grid operator to encourage the implementation of storage unit.

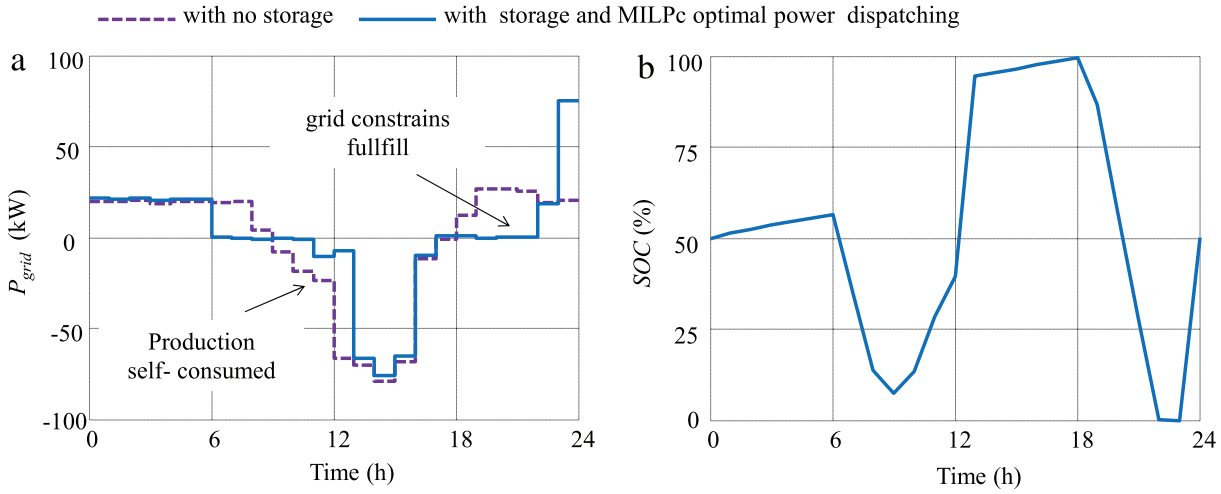

Fig. 4. Power profiles for the "spring day"—(a) P_{grid}—(b) SOC.

Table 3
Cost analysis for the "spring day".

	INIT	Storage and MILPc dispatching
Purchased energy (€)	94.5	23.3
Sold energy (€)	66.1	22.4
P_s exceeding penalized (€)	0.0	0.0
Total (€)	28.4	0.9

Table 4
Results of the different algorithms for the "winter day".

Algorithm	TR	CL	PSO	DP	DPa	MILPc
$C(\mathbf{P}^*_{\mathbf{ref}})$ (€)	346.4	344.5	346.1	343.5	344.6	345.3
CPU Time	1 h	5 h	2 h	2 h	10 min	3 s

3.3. "Winter day" and exceeding of subscribed power

The optimal power dispatching problem is now solved for the "winter day" but with no grid constraints considered. Once again the best result is found with the basic DP and a fine ΔSOC. The stochastic procedures are time consuming while the MILPc remains very fast with a similar cost (Table 4). As the amount of energy consumed is greater than in the previous case, the overall cost is much higher and the solution returned from the algorithms is different with less than a percent.

Fig. 5 shows the profiles for the power through the consumption meter with and without storage associated to the optimal dispatching. It can be seen on Fig. 5(a) that the exceeding of P_s is avoided and P_a remains below the limits thanks to the discharge of the storage unit from 3 to 6 p.m. (Fig. 5(b)).

The electrical bill is significantly reduced with the storage and MILPc dispatching with no penalties due to the P_s exceeding (Table 5). The overall discharge from 6 a.m. to 10 p.m. decreases the energy purchased from the grid during daily hours to generate an additional gain. The purchased energy is also reduced by the self consumption of the solar production while no surplus is sold.

4. Simulations over a whole year

4.1. Simulation "day after day"

Estimating the cost effectiveness of the microgrid from an optimal power dispatching strategy implies to run simulations of longer periods than a single day. Algorithms with expensive CPU times cannot be considered in that context.

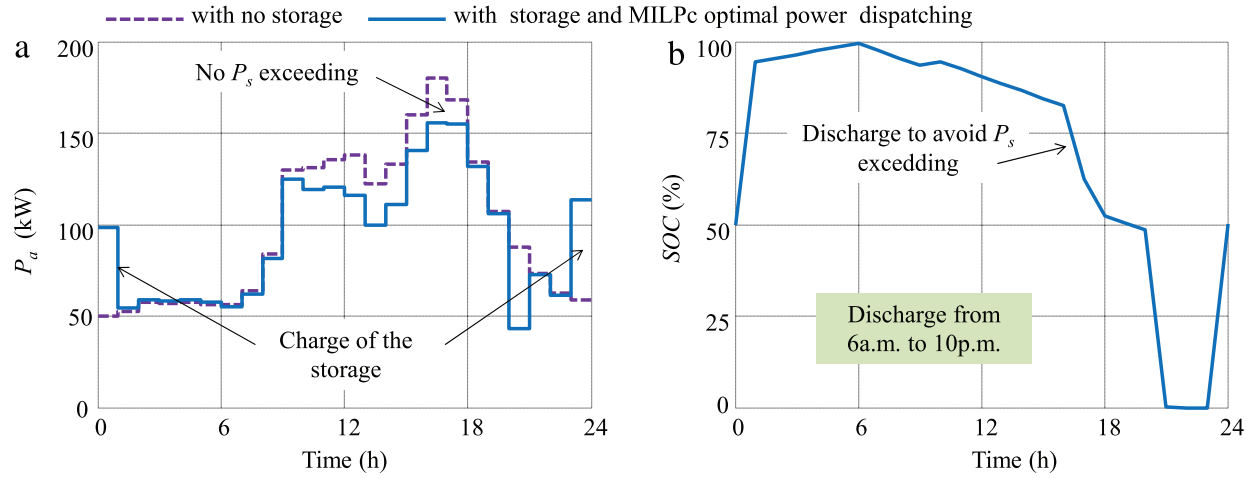

Fig. 5. Power profiles for the "winter day"—(a) P_{grid}—(b) *SOC*.

Table 5
Cost analysis for the "spring day".

	INIT	Storage and MILPc dispatching
Purchased energy (€)	369.9	345.3
Sold energy (€)	12.2	0.0
P_s exceeding penalized (€)	42.0	0.0
Total (€)	398.7	345.3

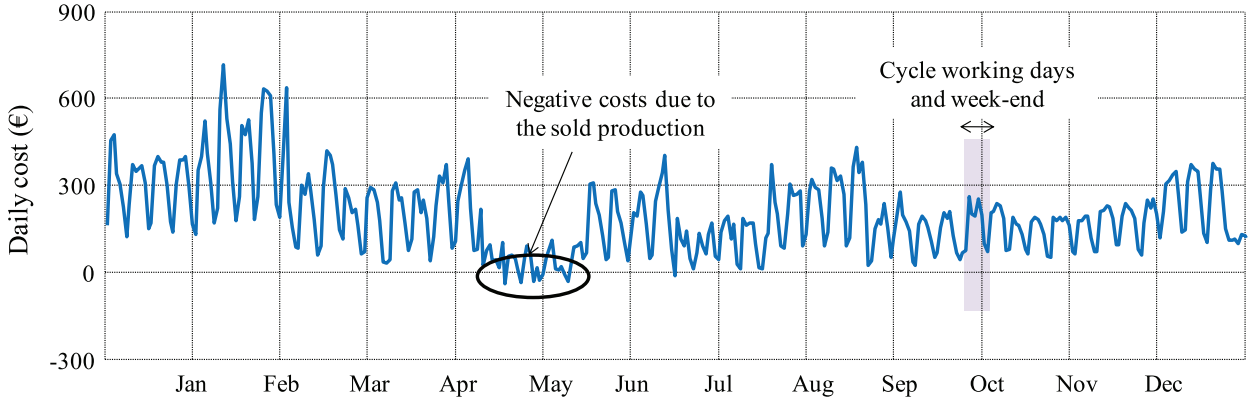

Fig. 6. Daily costs over a whole year after the MILPc optimization.

For instance the DPa needs around 10 min to simulate the microgrid management over a single day. Considering one year would last nearly three days of computation. The MILPc then appears to be the most suitable here, leading to the best compromise with regard to cost and computational time minimizations. It should be reminded that the chosen control is based on an optimal scheduling performed each day for the day ahead. Thus, to simulate a whole year, the MILPc procedure is successively carried out over 365 days. For each run, the storage has to return to the initial *SOC* value of 50% at the end of the day. The simulation of the microgrid management only lasts 15 min for the whole year. Fig. 6 illustrates the daily costs after the MILPc optimization with the previous price policy (i.e. $C_p = 17.0$ €/kWh from 6 a.m. to 10 p.m. and $C = 10$ c€/kWh otherwise, $C_s = 10.0$ c€/kWh and $C_{ex} = 14$ €/h) and the same sizes for the components (i.e. $E_{FS} = 100$ kWh and $P_{PV} = 175$ kWc) with no grid constraints.

With load and production profile for 365 days, the daily costs significantly differ depending on the period in the year with values up to 700 € and with a minimum at −30 € in a case where a gain is generated thanks to the sold production. The variation of the daily cost within a week is also visible in Fig. 6 between working days and week-end days due to consumption variation. The cost analysis of Table 6 compares a "INIT" case with neither storage nor

Table 6
Cost analysis for a whole year.

	INIT	Storage and MILPc dispatching
Purchased energy (k€)	97.0	71.3
Sold energy (k€)	16.3	1.5
P_s exceeding penalized (k€)	7.3	0.7
Total (k€)	88.0	70.5

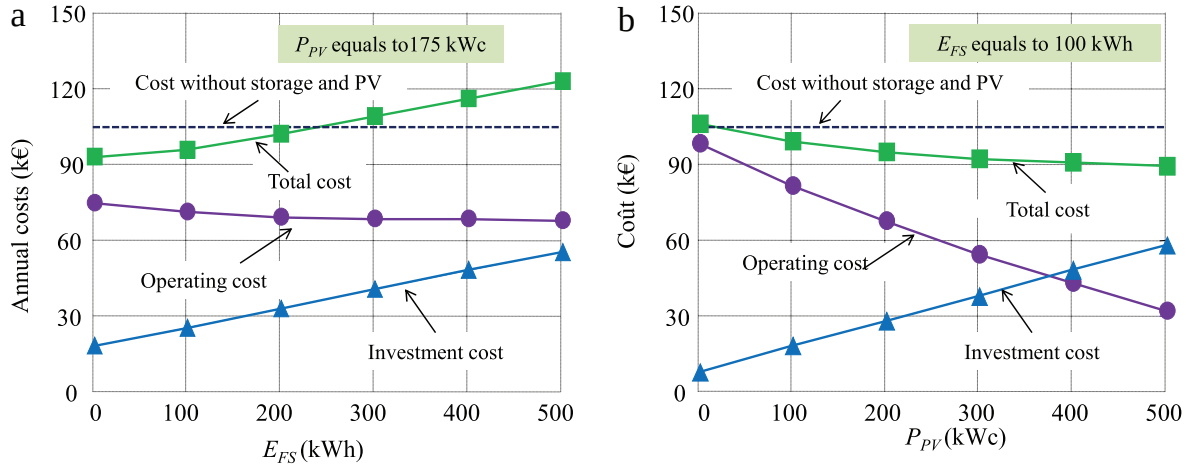

Fig. 7. Yearly cost considering the price of the components—(a) E_{FS} variable sizing—(b) P_{PV} variable sizing.

optimal dispatching (but with PV panels) and a situation after MILPc optimization for $E_{FS} = 100$ kWh. Without considering the investment cost, the overall electrical bill decreases from 20% with a significant reduction of the penalties for the exceeding of P_s due to the adapted management of the microgrid.

4.2. *Compromise between operating and investment costs*

The MILPc is now used to simulate the microgrid management over a whole year for different sizes of the flywheel storage (E_{FS}) and PV panels (P_{PV}). The operating cost is computed in each case and corresponds to the yearly electrical bill. In a context of optimal sizing of the system, the investment costs also have to be considered [2]. Thus the different sizes are evaluated by taking account of the cost of ownership related to the storage and the solar generator. PV arrays are associated with a cost of 2 €/Wc [19] and the flywheels with 1500 €/kWh [26]. A lifetime of 20 years is expected for the installation: it means that no replacements of these two devices are predicted during the 20 years of the microgrid operation.

Fig. 7 displays the costs of different sizes with reference to a case with no storage and no PV generator where all the consumed energy is purchased from the grid with no opportunity to reduce the exceeding of P_s. Firstly P_{PV} remains equal to 175 kWc while the nominal energy within the storage varies from 0 to 500 kWh. Increasing the size of the storage reduces the overall electrical bill but when E_{FS} is greater than 200 kWh, the annual total cost becomes penalized due to the price of the flywheels. The final electrical bill could even be worse than in a case with no storage and PV (Fig. 8(a)). On the contrary, the annual cost keeps decreasing when the power of the photovoltaic generator becomes greater. Indeed the operating cost is drastically reduced with an energy sold at 10 c€/kWh while the investment cost increase remains moderate (Fig. 8(b)).

4.3. *Sensitivity analysis and optimal sizing*

The fast MILPc method allows simulating many configurations of the microgrid. The previous section showed that a compromise has to be found between the investment cost and the operating cost to determine the most adapted sizing of the system components. Note that the optimum strongly depends on the price policies for both sold and purchased energies and it is also coupled with the cost of the different components. The yearly electrical bill also depends on the

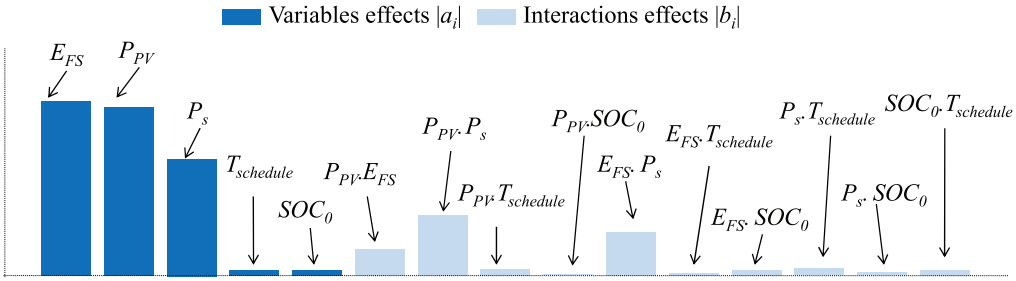

Fig. 8. Variable and interaction effects.

Table 7
Full factorial design of experiments.

$\mathbf{a_1 = x_1}$	$\mathbf{a_2 = x_2}$	$\mathbf{b_1 = x_2 x_1}$	$\mathbf{Y}$
$+1$	$+1$	$+1$	y_1
$+1$	-1	-1	y_2
-1	$+1$	-1	y_3
-1	-1	$+1$	y_4

value of P_s. Indeed P_s defines an annual subscription fee of 30.7 €/kVA. If it is too low, that cost would be reduced but the exceeding of subscribed power could be highly penalized. On the contrary a great value of P_s would decrease the exceeding but with a higher subscription fee.

Thus the subscribed power P_s is considered as an additional management parameter that could also be adapted in an optimal sizing procedure. The number of successive days $T_{schedule}$ on which the scheduling is extended is another possible variable. For $T_{schedule} = 1$ day as previously, 365 successive optimizations have to be performed to simulate a year. It should be noted that the computational time of the power flow scheduling strongly increases when the scheduling period becomes longer as the number of variables in the MILP problem is greater. The last studied variable denoted SOC_0 represents the initial and final SOC value in the optimization loop (50% previously). Bounds are arbitrary chosen for those five sizing variables:

- $0\,\text{kWh} < E_{FW} < 1500\,\text{kWh}$
- $0\,\text{kW} < P_{PV\_max} < 500\,\text{kW}$
- $150\,\text{kVA} < P_s < 250\,\text{VA}$
- $1\,\text{day} < T_{schedule} < 120\,\text{days}$
- $0\% < SOC_0 < 100\%$.

A sensitivity analysis is then performed using a full factorial design of experiments [1]. Starting from a reduced number of tested points, that study aims at finding the most influent variables with regards to the objective function (i.e. the yearly cost of the system here). As illustrated in Eq. (27) with a simple model for a two parameters function ($y = f(x_1, x_2)$) the effect of each variable x_i is identified to a coefficient a_i. The first order interactions between variables $x_i \cdot x_j$ are associated to weight coefficients b_i. In Eq. (27), $\hat{y}$ is the average value of the function with the N different tested points y_i given by the design of experiments and written in a vector $\mathbf{Y}$.

$$y = \hat{y} + a_1 \times x_1 + a_2 \times x_2 + b_1 \times x_1 \cdot x_2 \tag{27}$$

$$\begin{cases} a_i = \mathbf{a_i^T} \cdot \mathbf{Y}/N \\ b_i = \mathbf{b_i^T} \cdot \mathbf{Y}/N. \end{cases} \tag{28}$$

Table 7 is then used to generate vectors $\mathbf{a_i}$ and $\mathbf{b_i}$ with coefficients depending on the values of variables that are at their higher ($+1$) or lower (-1) bounds. The weight a_i and b_i are eventually computed using Eq. (28).

For five parameters, as for the studied problem, the absolute values of all coefficients are plotted in Fig. 8. The corresponding parameters (effect/interactions) are underlined. The coefficients referring to the values of E_{FS}, P_{PV}, and P_s appear to be the most influent. In a first approximation, only those three variables could be considered when studying different sizing cases.

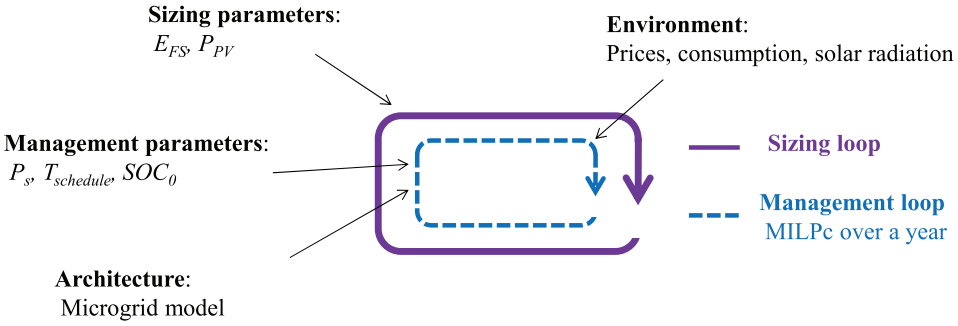

Fig. 9. Optimal dispatching in a sizing loop.

Finally, the fast control algorithm may offer the ability of achieving systemic design of microgrids integrating sizing optimization loop with power dispatching optimization by taking account of system environment and requirements [25]. The whole process could be represented by Fig. 9 with the MILPc procedure performed over a year to estimate the operating cost that has to be added to the investment prices for a tested sizing. The algorithm of the sizing loop would have to explore the search space within the bounds in order to find the values for the sizing and management parameters that would minimize the annual cost for a given price context. Further developments on that topic have been recently proposed in [21].

5. Conclusion

The study carried out in this article aims at proposing a fast procedure in terms of computation time that could be used to investigate cost-effectiveness of a microgrid with storage. In previous works, efficient algorithms have been developed to perform the daily scheduling of power flows. However, the main drawbacks of these methods reside in their computational times that become prohibitive if the microgrid has to be simulated over a long period of time. To overcome this problem, a fast optimization approach based on MILP has been proposed. This approach consists in two successive steps. Firstly, a coarse linear model of the microgrid is exploited to solve the optimal dispatching with a classical MILP algorithm. Secondly, control references optimized with the coarse model are adapted in order to comply with a finer model of the microgrid which takes account of nonlinear features (i.e. efficiencies). The performance of this approach with regard to energy cost minimization and computational time reduction has been shown on two particular test days. The procedure MILPc revealed itself satisfying to consider grid constraints and exceeding of subscribed power. Moreover, the fast CPU time resulting from this optimal dispatching method has allowed us to simulate the microgrid over a whole year and to investigate several configurations. The obtained results have shown in an optimal sizing context a compromise has to be found between the operating and the investment costs of the components. Future studies will be focused on the same issue with other kind of storage technologies such as Li-ion batteries for which cycling effect would have to be included in the cost function. Finally, the optimal sizing process would be completed with an adapted sizing algorithm that would allow finding the best configurations depending on the considered price policies.

Acknowledgments

This study has been carried out in the framework of the SMART ZAE national project supported by ADEME (Agence de l'Environnement et de la Maîtrise de l'Energie). The authors thank the project leader INEO-SCLE-SFE and partners LEVISYS and CIRTEM.

References

[1] M. Antonio, T. Clé, J. Maria, J. Policarpo, Design of experiments for sensitivity analysis of voltage sags variables, in: 15th International Conference on Harmonics and Quality of Power, Hong-Kong, China, 2012, pp. 398–402.

[2] S. Bahramirad, W. Reder, A. Khodaei, Reliability-constrained optimal sizing of energy storage system in a microgrid, Trans. Smart Grid 3 (2012) 2056–2062.

[3] K. Basu, V. Debusshere, S. Bacha, Appliance usage prediction using a time series based classification approach, in: Symposium du Génie Electrique, Paris, France, 2014.

[4] P. Bertsekas, Dynamic Programming and Optimal Control, second ed., Athena Scientific, 2000.
[5] J. Bisshop, Optimization Modeling, Paragon Decision Technology, 2012.
[6] S. Bolognani, G. Cavraro, F. Cerruti, A. Costabeber, A linear dynamic model for microgrid voltages in presence of distributed generations, in: International Workshop on Smart Grid Modeling and Simulation, Brussels, Belgium, 2011, pp. 31–36.
[7] A. Campoccia, L. Dusonchet, E. Telaretti, G. Zizzo, Feed-in tariffs for gridconnected PV systems: the situation in the European community, in: PowerTech, Lausanne, Switzerland, 2007, pp. 1981–1986.
[8] G. Celli, F. Pilo, G. Pisano, V. Allegranza, R. Cicoria, A. Iaria, Meshed vs. radial MV distribution network in presence of large amount of DG, in: Power Systems Conference and Exposition, 2004.
[9] T.F. Coleman, Y. Li, An interior trust region approach for nonlinear minimization subject to bounds, SIAM J. Optim. 6 (1996) 418–445.
[10] C.M. Colson, A review of challenges to real-time power management of microgrids, in: Power & Energy Society General Meeting, Calgary, Canada, 2009, pp. 1–8.
[11] C. Darras, S. Sailler, C. Thibault, M. Muselli, P. Poggi, J.C. Hoguet, S. Melsco, E. Pinton, S. Grehant, F. Gailly, C. Turpin, S. Astier, G. Fontès, Sizing of photovoltaic system coupled with hydrogen/oxygen storage based on the ORIENTE model, Int. J. Hydrog. Energy 35 (2010) 332–333.
[12] R. Gilbert, C. Moler, R. Schreiber, Sparse matrices in matlab: design and implementation, J. Matrix Anal. Appl. 13 (1992) 333–356.
[13] P. Haessig, B. Multon, H. Ben Ahmed, S. Lascaud, P. Bondon, Energy storage sizing for wind power: impact of the autocorrelation of day-ahead forecast errors, Wind Energy (2013).
[14] H. Kanchev, F. Colas, V. Lazarov, B. Francois, Emission reduction and economical optimization of an urban microgrid including dispatched PV-based active generators, Trans. Sustainable Energy 5 (2014) 1397–1405.
[15] J. Kennedy, R. Eberhart, Particle swarm optimization, in: International Conference on Neural Networks, 1995, pp. 1942–1948.
[16] B. Meindl, M. Templ, Analysis of Commercial and Free and Open Source Solvers for Linear Optimization Problems, Vienna University of Technology, 2012.
[17] S. Pazouki, S. Member, M. Reza Haghiafm, Market based operation of a hybrid system including wind turbine, solar cells, storage device and interruptable load, in: Conference on Electrical Power Distribution Networks, Kermanshah, Iran, 2013.
[18] A. Petrowski, A clearing procedure as niching method for genetic algorithms, in: International Conference on Evolutionnary Computation, Nagoya, Japan, (11), 1996, pp. 798–803.
[19] S. Reichelstein, M. Yorston, The prospects for cost competitive solar PV power, Energy Policy 55 (2013) 117–127.
[20] Y. Riffoneau, S. Bacha, F. Barruel, S. Ploix, Optimal power flow management for grid connected PV systems with batteries, Trans. Sustainable Energy 2 (2011) 309–319.
[21] R. Rigo Mariani, B. Sareni, X. Roboam, Optimization methodologies for the power management and sizing of a microgrid with storage, in: Symposium du Génie Electrique, Paris, France, 2014.
[22] R. Rigo-Mariani, B. Sareni, X. Roboam, S. Astier, J.G. Steinmetz, E. Cahuet, Off-line and on-line power dispatching strategies for a grid connected commercial building with storage unit, in: 8th IFAC Power Plant and Power Systel Control, Toulouse, France, 2012.
[23] R. Rigo-Mariani, B. Sareni, X. Roboam, C. Turpin, Optimal power dispatching in smart microgrids with storage, Renew. Sustainable Energy Rev. 40 (2014) 649–658.
[24] Y. Ru, J. Kleissl, S. Martinez, Storage size determination for grid-connected photovoltaic systems, Trans. Sustainable Energy 4 (2013) 1–13.
[25] J.W. Whitefoot, A.R. Mechtenberg, D.L. Peters, P.Y. Papalambros, Optimal component sizing and forward-looking dispatch of an electrical microgrid for energy storage planning, in: International Design Engineering Technical Conferences and Computers and Information in Engineering Conference, Washington, United-States, 2011.
[26] Website—American Flywheels Manufacturer. www.beaconpower.com.
[27] Website—French Power Supllier. www.edf.com.
[28] S. Yeleti, F. Yong, Impacts of energy storage on the future power system, in: North American Power Symposium, Arlington, United-States, 2010.